

OPEN ACCESS

Evidence for graphene growth by C cluster attachment

To cite this article: Elena Loginova *et al* 2008 *New J. Phys.* **10** 093026

View the [article online](#) for updates and enhancements.

You may also like

- [Directionality reduces the impact of epidemics in multilayer networks](#)
Xiangrong Wang, Alberto Aleta, Dan Lu et al.
- [Magnetoconductivity of Dirac fermions in graphene under charged impurity scatterings](#)
Xin-Zhong Yan and C S Ting
- [Cooperative interplay between impurities and charge density wave in the phase transition of atomic wires](#)
Hyungjoon Shim, Geunseop Lee, Jung-Min Hyun et al.

Evidence for graphene growth by C cluster attachment

Elena Loginova¹, Norman C Bartelt¹, Peter J Feibelman²
and Kevin F McCarty^{1,3}

¹ Sandia National Laboratories, Livermore, CA 94550, USA

² Sandia National Laboratories, Albuquerque, NM 87185, USA

E-mail: mccarty@sandia.gov

New Journal of Physics **10** (2008) 093026 (16pp)

Received 17 June 2008

Published 25 September 2008

Online at <http://www.njp.org/>

doi:10.1088/1367-2630/10/9/093026

Abstract. Using low-energy electron microscopy (LEEM), we have measured the local concentration of mobile carbon adatoms from which graphene sheets form on a Ru(0001) surface, and simultaneously, the growth rates of individual graphene islands. Graphene crystal growth on Ru differs strikingly from that of two-dimensional metal islands on metals: (i) C adatoms experience a large energy barrier to attaching to graphene step edges, so adatom diffusion does not limit growth. (ii) The supersaturations needed for appreciable growth rates are comparable to those required to nucleate islands. (iii) The growth rate is a highly nonlinear function of supersaturation, with a large activation energy (2.0 ± 0.1 eV). Our analysis suggests that graphene grows by adding rare clusters of about five atoms rather than adding the abundant monomers (adatoms). Knowing the growth mechanism and monitoring the supersaturation, we can control the pattern of growing graphene sheets.

³ Author to whom any correspondence should be addressed.

Contents

1. Introduction	2
2. Methods	3
2.1. Measuring local concentrations of C adatoms using electron reflectivity	3
2.2. Methods for first-principles calculations	4
3. Results and discussion	5
3.1. C adatom concentration in equilibrium with graphene	5
3.2. C adatom concentrations for graphene nucleation and growth	7
3.3. Nonlinear graphene growth with C adatom supersaturation	8
3.4. Model of graphene growth by C-cluster attachment	10
3.5. Microscopic interpretation of cluster-attachment kinetics	11
3.6. Controlling graphene nucleation by monitoring C adatom supersaturation	13
4. Summary	14
Acknowledgments	14
References	14

1. Introduction

The growth of graphitic carbon plays a large role in long-standing problems, such as the formation of soot in combustion [1] and the poisoning (coking) of catalysts [2]. Since carbon nanotubes are usually grown from metal catalysts [3], considerable effort has been devoted to carbon growth on metal surfaces [4]. Currently much attention is being given to single layers of graphite, i.e., graphene, because of its novel and potentially useful electronic properties [5]–[9]. Owing to this interest, the structure and defects of graphene sheets have been now characterized on many surfaces [10]–[17].

However, the ability to control graphene formation is primitive, in part, because the growth mechanism is largely unexplored experimentally. Many basic questions remain unanswered. In general, the growth rates of two-dimensional crystals, such as graphene can be limited by surface diffusion or attachment, that is, by the rate at which deposited atoms diffuse towards the growing crystal or the rate at which these atoms attach to the crystal. Here, we answer such questions by using low-energy electron microscopy (LEEM) to study how graphene nucleates and grows on the transition-metal ruthenium (Ru).

We chose Ru(0001) as a substrate because it supports the growth of large epitaxial graphene sheets [8, 11, 15], and because the Ru electronic band structure is such that low-energy electrons reflect strongly from the (0001) surface [18]. We use the latter effect for measuring the local, absolute concentration of mobile carbon adatoms that surround growing graphene islands, and thereby find that a large supersaturation of carbon adatoms is needed to nucleate and grow graphene. These observations establish that graphene growth from vapour-deposited carbon is controlled by the rate at which atoms attach to the graphene step edges. In fact, the energy barrier against atom attachment is so large that crystal growth is not in the linear, close-to-equilibrium growth regime commonly observed on metal and semiconductor surfaces. Our analysis suggests that the nonlinear kinetics results from growth by addition of rare clusters of about five atoms rather than of far more abundant monomers (adatoms). Thus, the standard Kossel crystal model of growth [19] is not appropriate for graphene. By considering the results

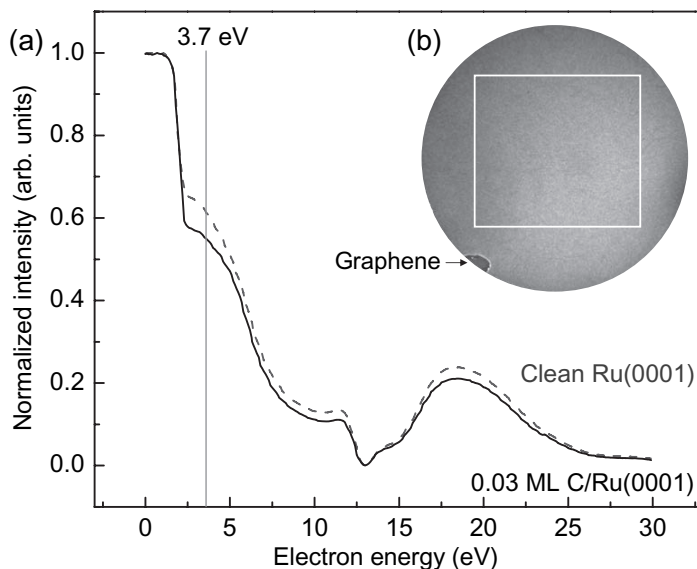


Figure 1. (a) Electron reflectivity as a function of incident electron energy for clean Ru(0001) (dashed line) and covered with the 0.032 ML of C adatoms (solid line) in equilibrium with graphene at 980 K; (b) LEEM image ($46\ \mu\text{m}$ field-of-view) with one (labelled) graphene island. The box shows the graphene-free region analysed in (a).

of various density functional theory (DFT) calculations [20], we attribute the large barrier to the characteristic of graphene to be weakly bound to a substrate, relative to individual C atoms. That is, growing a crystal by moving a C monomer several \AA in height from the substrate to the graphene layer is energetically difficult. Finally, we show that the large barrier to growth can be useful; it allows the graphene morphology to be controlled by monitoring and varying the C supersaturation.

2. Methods

2.1. Measuring local concentrations of C adatoms using electron reflectivity

All measurements were conducted under ultrahigh-vacuum conditions in a LEEM. Carbon was deposited onto a Ru(0001) surface from a high-purity carbon rod heated by electron bombardment. The deposition rate was controlled by precisely regulating power to the evaporator. The Ru(0001) surface was cleaned by cycles of exposure at $\sim 800\ \text{K}$ to O_2 at 1×10^{-8} Torr and flashing to $\sim 1660\ \text{K}$ in vacuum. By scrupulously depleting the crystal bulk of carbon and only depositing carbon at temperatures low enough that carbon diffusion into Ru is negligible, we ensured that carbon segregating from Ru did not contribute to the graphene growth. Temperature was recorded from a tungsten–rhenium type-C thermocouple spot welded to the crystal side. The concentration of carbon adatoms was measured from the change in electron reflectivity [21], as determined from the intensity (brightness) of LEEM images formed from the specularly reflected electron beam. This approach allows imaging the growth of graphene islands, while simultaneously measuring the local reflectivity. Figure 1 shows how carbon adatoms decrease the efficiency of electron reflectivity as a function of incident electron

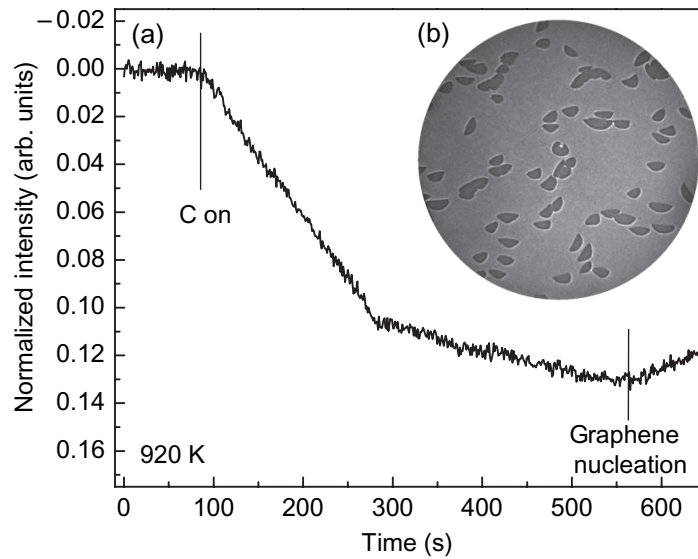


Figure 2. (a) Electron reflectivity, $1 - I/I_0$, normalized to the initial value, during C deposition at two constant rates (evaporator power changed at 281 s) at 920 K. This result establishes that the reflectivity change is a simple linear function of the C adatom concentration. (b) LEEM image ($46 \mu\text{m}$ field-of-view) taken at equilibrium, at 2400 s.

energy. All adatom concentration measurements were made using electrons with incident energy 3.7 eV, close to the energy of maximum sensitivity.

At a constant rate of carbon deposition, the reflectivity decreases linearly with time (figure 2). The linear electron reflectivity change was converted to an absolute C adatom coverage using the elapsed time to grow a measured coverage of graphene at constant deposition flux. The final fractional surface coverage of graphene islands was determined by averaging the coverages from 20 LEEM images of different areas. After correcting self-consistently for the small fraction of the deposited C that is adatoms at equilibrium, we find that the adatom coverage equals $0.223 \times \frac{I_0 - I(t)}{I_0}$ ML, where I_0 is the image intensity measured before C deposition, and $I(t)$ is the intensity at time t . Concentrations are given in monolayers (ML), where 1 ML equals the area density of the carbon in graphene on Ru(0001).

The dependence of graphene growth rate on adatom concentration was measured in two ways. Firstly, graphene islands were imaged soon after nucleation, as they grew from the initially supersaturated adatom gas, until the deposition flux was halted and the equilibrium established (as in figure 3). Alternatively, an island initially at equilibrium (i.e., no growth flux) was imaged as the deposition flux was started, increased, decreased and finally stopped (see figure 5(a)). To determine graphene growth-edge velocities below 850 K, isolated islands were first nucleated at higher temperatures, where achieving a lower nucleation density is easier.

2.2. Methods for first-principles calculations

We used VASP [22, 23], in the PW91 generalized gradient approximation [24], for energy optimization, with electron–core interactions treated in the projector augmented wave approximation [25, 26]. With the VASP plane wave basis cut off at 700 eV, the C adatom

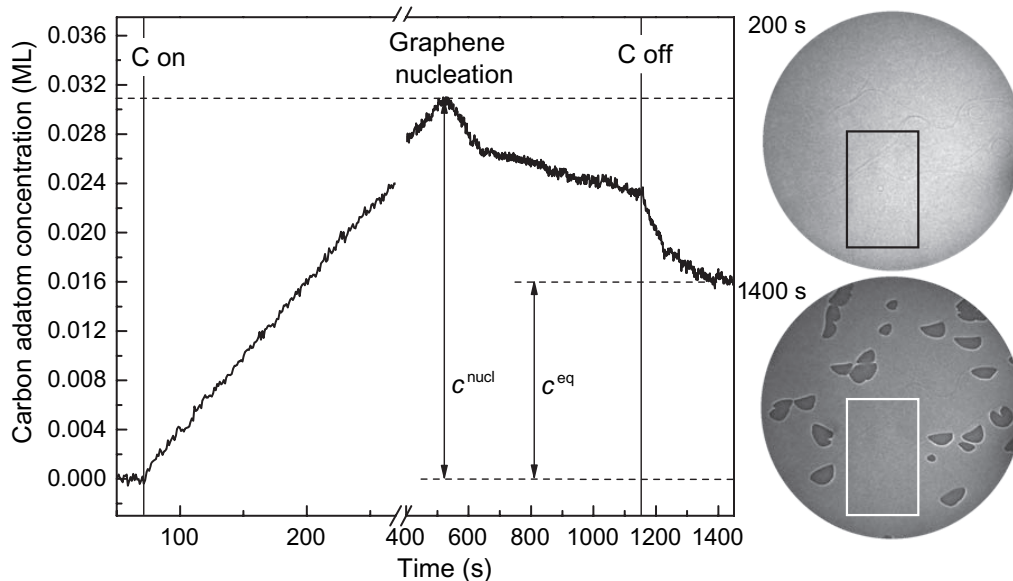


Figure 3. The C adatom concentration in equilibrium with graphene measured from electron reflectivity at 940 K (left panel). The LEEM images ($46 \mu\text{m}$ field-of-view) taken at 200 s and 1400 s (right panel). Boxes mark the graphene-free region where the C monomer concentration was determined. c^{nucl} and c^{eq} are the monomer concentrations needed to nucleate graphene and be in equilibrium with graphene, respectively.

formation energy was computed by comparing the binding of a C atom in an hcp hollow site on a seven-layer Ru(0001) slab in a $2\sqrt{3} \times \sqrt{3} - R30^\circ$ supercell to the binding per C atom in a single graphene layer (C binding in an fcc hollow on Ru was found to be ~ 0.7 eV weaker). In the Ru supercell calculations, the surface brillouin zone (SBZ) was sampled with a 9×9 set of equal-spaced k-points, the atoms of the lower three Ru layers were fixed in relative positions consistent with a PW91, bulk Ru geometry optimization, and correction was made for unphysical fields associated with adsorbing C atoms only on the upper surface (cf [27]). For the primitive graphene cell, an 18×18 SBZ sample was used. Repeating the calculations with a thinner Ru slab, a larger supercell or a coarser SBZ sample yielded a numerical confidence level of better than 10 meV in the computed energies.

3. Results and discussion

3.1. C adatom concentration in equilibrium with graphene

Figure 3 illustrates the precise measurement of local C adatom concentration via changes in electron reflectivity. The mobile C adatom concentration increases linearly with time as elemental C is deposited on an initially clean Ru surface. Once the concentration reaches a critical value, c^{nucl} , graphene islands nucleate. Graphene growth then consumes adatoms, decreasing their concentration. After C deposition is stopped (1150 s), the monomer concentration decreases slowly, until equilibrium with graphene is established.

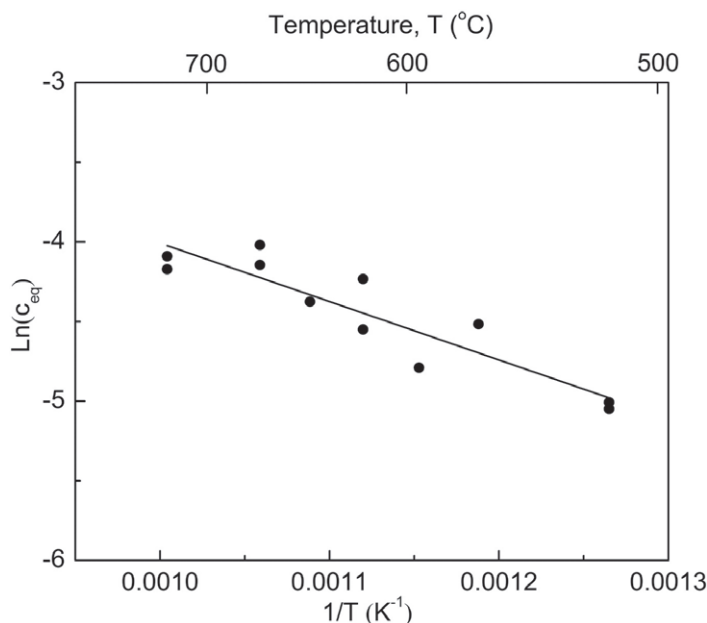


Figure 4. Temperature dependence of the C adatom concentration in equilibrium with graphene, c^{eq} , measured using the procedure shown in figure 3.

A first inference from figure 3 is that the C adatom concentration in equilibrium with graphene sheets is substantial: $c^{\text{eq}} = 0.016 \text{ ML}$ at 940 K. This value is set by the formation enthalpy of a carbon monomer, E_{form} i.e., the energy cost of carbon atom detachment from the graphene sheet followed by adsorption on the metal. Since, in the reverse process, C atoms must break their bonds to the metal before attaching to a graphene sheet, the formation enthalpy is a key ingredient of the energy landscape governing graphene growth. The large equilibrium concentration of C adatoms suggests that E_{form} is small.

We confirm this expectation by determining E_{form} from the temperature dependence of c^{eq} , measured using the procedure of figure 3. As anticipated, the carbon monomer concentration needed to equilibrate relatively large graphene islands increases with increasing temperature. Assuming

$$c^{\text{eq}} \propto e^{-(E_{\text{form}}/kT)}, \quad (1)$$

the Arrhenius plot in figure 4 gives $E_{\text{form}} = 0.33 \text{ eV} \pm 0.10 \text{ eV}$. This low value may seem surprising given how strongly carbon is bound in graphene. However, the DFT calculations show that C is also strongly bound to the Ru surface: we calculate a formation energy from a free-standing graphene sheet to be 0.27 eV (see methods). Graphene on Ru forms a moiré with an (11×11) unit cell [11, 15, 20]. A recent x-ray diffraction study suggested a (25×25) moiré [28]. Recent DFT calculations give 0.04 eV per C atom attraction between the graphene moiré and the Ru substrate [20]. Thus, the energy E_{form} of forming an adatom from graphene on Ru is $0.27 + 0.04 = 0.31 \text{ eV}$. The good agreement of this number with experiment supports the claim that we are indeed monitoring the C monomer concentration, and suggests that DFT has not underestimated significantly the graphene–Ru interaction. STM observations of similar concentrations of monomers on quenched samples are also consistent with our claim [29].

Regarding energetic barriers to growth, the DFT calculations suggest that C monomers might not have a low-energy pathway to attach to graphene sheet edges: the monomer's calculated position is 1.0 Å above the surface plane of Ru atoms, while the graphene sheet is found by Wang *et al* [20] to be strongly corrugated with a height varying from 2.2 Å to 3.7 Å [20]⁴. Low barriers come from transition paths in which bond formation and bond breaking happen at the same time. For a C monomer, bound to three Ru atoms, to form several new bonds to the higher lying graphene edge as the C–Ru bonds break might be difficult. Binding of graphene edge atoms to the Ru substrate or rebonding of the graphene edge (as proposed to occur in [2, 30, 31]) would complicate an understanding of the attachment event. However, our LEEM results discussed below imply that monomer attachment is indeed sufficiently difficult as to be unimportant in graphene growth.

3.2. C adatom concentrations for graphene nucleation and growth

The second notable aspect of our LEEM data is the large supersaturation needed for graphene islands to nucleate and grow. In figure 3, islands appear only when the monomer concentration is about twice the equilibrium concentration ($c^{\text{nucl}} \approx 2c^{\text{eq}}$) and growth is quite slow even when the local monomer concentration, c , is high relative to c^{eq} (e.g., $c = 1.5$ to $1.9 \times c^{\text{eq}}$ during C deposition in figure 3). Usual theories of growth from dense adatom 'seas' assume that deviations from equilibrium are small, so that growth occurs as a small bias between the random attachments and the detachments [32]. Indeed, the adatom concentration during metal film growth and even nucleation is so small that we have not been able to measure them even in a system where the equilibrium adatom concentration is comparable to the C concentration here and even though the electron reflectivity technique can be sensitive to as little as 10^{-4} ML of adatoms [21]. In contrast, graphene only grows at appreciable rates far from equilibrium. So for example, the Gibbs–Thomson driving force for flow of material from small islands to large islands to decrease total edge length is too small to lead to appreciable island size coarsening. And indeed, we never observed such Ostwald ripening in this system at any temperature below the temperature where C dissolves into Ru. Again, this is in contrast to metal and semiconductor systems where island ripening is common [33].

Another important feature of graphene growth is that the monomer concentration is always uniform across the graphene-free Ru terraces. Figure 5(a) shows a LEEM image of graphene islands growing during C deposition. Figure 5(b) shows the corresponding map of C monomer concentration as determined using the method of section 2.1. The profile in ratio c/c^{eq} units measured along the black line (see figure 5(b)) illustrates the homogeneity of the C monomer concentration. The lack of observable diffusion gradients directly implies that graphene growth is not limited by the rate of monomer diffusion on the terraces, and that a large energy barrier impedes monomer attachment to the edge of graphene sheets. Consistently, equilibrating adatoms and islands is extremely slow. In figure 3, for example, the islands grow by consuming the supersaturation for ~ 200 s after the deposition flux has stopped. This behaviour differs again from what occurs in epitaxial metal crystal growth, where an adatom attaching to a step edge faces no extra barrier. These observations also contradict assumptions commonly made about graphene and nanotube growth on metal surfaces [3, 34].

⁴ A much smaller experimental estimate of 1.45 Å from [8] assumes a simplified (1 × 1) structure that does not allow for the complexity of the (11 × 11) unit cell structure calculated in [20].

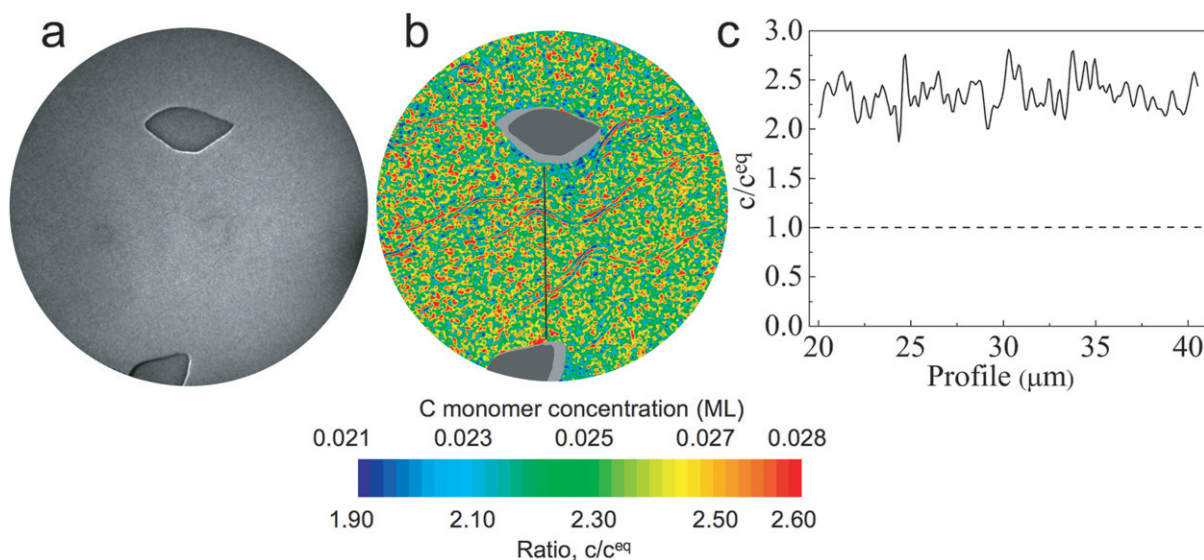


Figure 5. (a) LEEM image ($46\ \mu\text{m}$ field-of-view) at $t = 403\ \text{s}$ during carbon deposition at $980\ \text{K}$; (b) corresponding C monomer concentration map obtained from averaging ten LEEM images taken between 393 and $403\ \text{s}$ and applying a $3\ \text{pixel} \times 3\ \text{pixel}$ smoothing function. The graphene islands (black) from image (a) are inserted for reference. A narrow band (grey) around the islands has been removed from the map where the image intensity is skewed by a local lensing effect caused by the difference in work function between graphene and Ru; (c) c/c^{eq} ratio measured between two islands along the black line indicated in (b).

3.3. Nonlinear graphene growth with C adatom supersaturation

Having shown that we can measure C monomer concentrations accurately, we now turn to the central issue of this paper—understanding how the graphene growth rate depends on monomer concentration. This knowledge will give us insight into the microscopic processes underlying the exceptional behaviour just discussed. The essential measure of graphene growth rate is the velocity v at which the edges of graphene sheets advance as a function of supersaturation, $c - c^{eq}$. For islands, the average edge velocity v is equal to $(1/P)dA/dt$, where P and A are the island perimeter and area, respectively⁵. We measure both these quantities from the LEEM images, while simultaneously determining the C adatom concentration adjacent to the island. Figure 6 shows the experimental procedure. A graphene island, initially in equilibrium with C monomers at $c^{eq} = 0.019\ \text{ML}$, was taken out of equilibrium by depositing carbon on the surface. Figure 6(a) shows how the adatom concentration changed as the evaporator power (figure 5(a)) was subsequently increased in steps, decreased in steps, and finally turned off at $620\ \text{s}$. After $1000\ \text{s}$, the C adatom concentration has returned to its equilibrium value of $0.019\ \text{ML}$ and the island has grown (see inserts to figure 6(b)). Figure 6(c) shows that the edge velocity v , measured from island area and perimeter, of different islands are the same, even though the islands have

⁵ Because the graphene islands grow away from substrate step edges [8], the step velocity along some of each island periphery is zero. However, because the shapes of all the islands are similar and remain roughly constant in time, the difference between the average velocity and the velocity of the moving edge is a constant factor that does not affect our analysis.

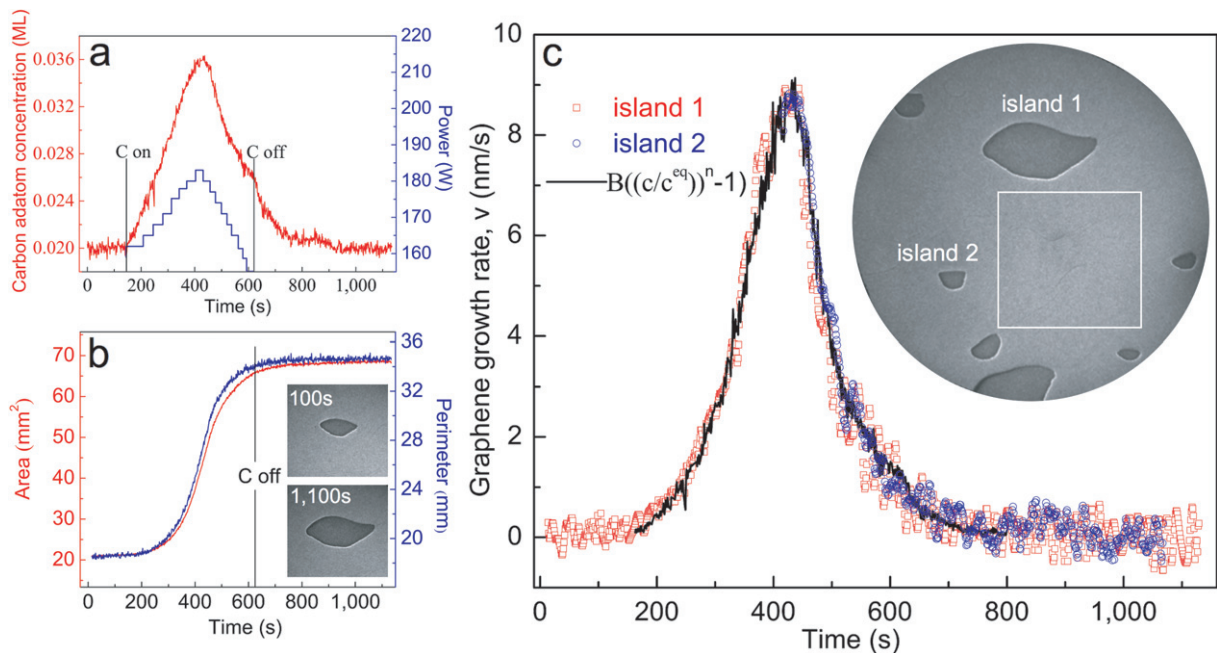


Figure 6. (a) C adatom concentration (red) during graphene growth at 980 K with variable C flux obtained by changing evaporator power (blue). C deposition ended at 620 s. (b) Area and perimeter of the graphene island shown in the LEEM images ($25 \mu\text{m}$ field-of-view) growing at 980 K. (c) Two islands have the same graphene step velocity $v = (1/P)dA/dt$ even though they nucleated at different times, have different sizes and different configurations of neighbouring islands. Thus, v is completely determined by the local C adatom concentration, independent of island size and environment. The black line is a fit of the step velocity of island 1 to equation (3). Graphene monomer concentration was measured in the indicated white box shown in the LEEM image ($46 \mu\text{m}$ field-of-view) taken at equilibrium (at 1075 s).

different sizes and different configurations from neighbouring islands. Thus, v measures the intrinsic growth rate.

Figure 7 shows that the growth velocity v is a highly nonlinear function of the supersaturation. Typically, the edge velocity in film growth is assumed to be proportional to the supersaturation: $v = m(c - c^{eq})$, where the step mobility m is proportional to the rate at which C in the adatom sea is attaching (and detaching) at each point along the step edge *in equilibrium*. (In the simplest model of growth the attachment rate is proportional to the number of monomers, and the detachment rate is taken to be independent of monomer concentration. The growth velocity, which is the difference between attachment and detachment rates, is then linear in monomer concentration regardless of the size of the attachment barrier.) This assumption has successfully modelled step motion in crystal growth from vapour deposition (e.g., silicon [32, 35]) and in solution [36]. In the next section, we propose a model to explain our puzzling observation of nonlinear kinetics by assuming monomers do not directly attach to the step edge.

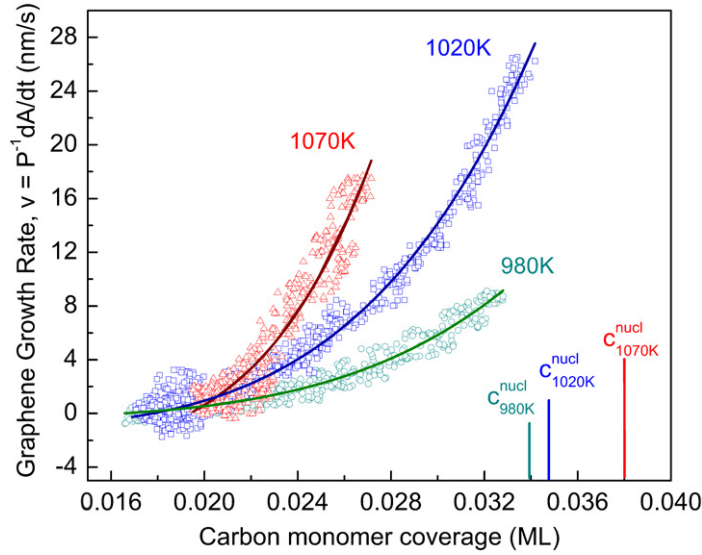


Figure 7. Island growth rate as a function of monomer concentration. The solid lines are fits to equation (3) with three parameters: B , c^{eq} and n . At 980, 1020 and 1070 K, $n = 4.9$, 4.8 and 5.2, respectively. The vertical lines show the adatom concentration at island nucleation, c^{nucl} .

3.4. Model of graphene growth by C-cluster attachment

One way to rationalize the nonlinear kinetics is to suppose that the barrier to monomer attachment is much larger than the barrier for a cluster of n C atoms to form and then attach. (Physical interpretations of the monomer barrier are discussed in section 3.5.) The density of these clusters in the supersaturated adatom sea depends exponentially on the energy difference between n isolated C adatoms and the energy needed to form the n -atom cluster E_n :

$$c_n = e^{n\mu/kT - E_n/kT} = \left(\frac{c}{c^{\text{eq}}}\right)^n e^{-E_n/kT}, \quad (2)$$

where the monomer sea is taken to be an ideal lattice gas with C chemical potential

$$\mu = kT \ln(c/c^{\text{eq}}). \quad (3)$$

If we now assume that the growth velocity is proportional to how far this cluster concentration is out of equilibrium, we obtain

$$v = m_n(c_n - c_n^{\text{eq}}) = m_n e^{-E_n/kT} \left[\left(\frac{c}{c^{\text{eq}}}\right)^n - 1 \right] = B \left[\left(\frac{c}{c^{\text{eq}}}\right)^n - 1 \right]. \quad (4)$$

For the case when $n = 1$, the expected linear kinetics of monomers is reproduced. Fitting of the experimental data was performed varying three parameters: B , c^{eq} and n . (Values of c^{eq} obtained by the fits are equal, within experimental uncertainty, to those directly measured in experiments described in section 3.1, illustrating the self-consistency of our data and model.) Figure 7 shows that this model faithfully describes a very large amount of experimental data. Furthermore, figure 6(c) shows that the model of equation (4) accurately describes the growth rate of islands of greatly different size and with different configurations of neighbouring islands. For eight datasets over the temperature range from 740 to 1070 K, the best fits to equation (4) give $n = 4.8 \pm 0.5$, where the error is the standard deviation.

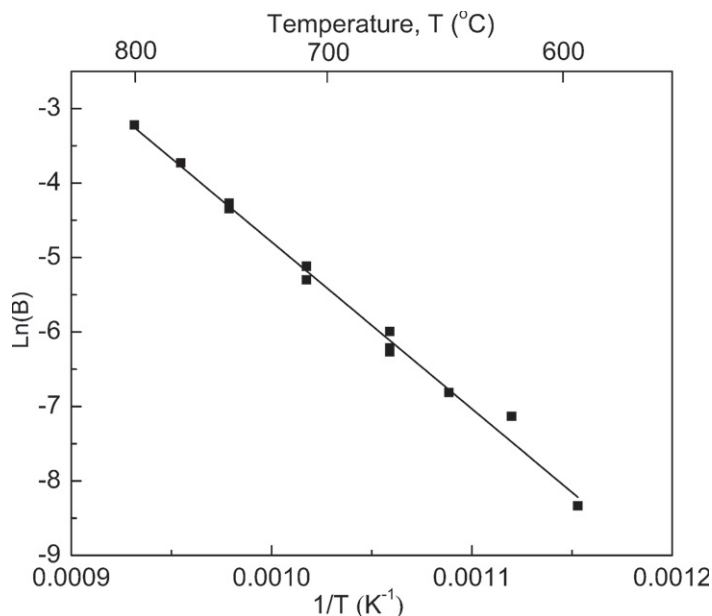


Figure 8. Graphene growth rate assuming five-atom-cluster kinetics (equation (4) with $n = 5$).

In this picture, as the density of monomers in the adatom sea increases, clusters of five C atoms begin to form with appreciable probability and these can exchange with the graphene edge. An Arrhenius plot of the fitted values of B (see figure 8) shows that the graphene growth rate, which is limited by the kinetics of cluster addition, gives an activation energy of $2.0 \text{ eV} \pm 0.1 \text{ eV}$. This energy is the sum of E_n and the energy controlling cluster attachment/detachment. (The latter is the temperature dependence of m_n .) An activation energy for carbon growth on metal surfaces in the range of 1 to 2 eV is often taken to imply that growth is limited by C diffusion through the metal substrate or catalyst [37]. Here, we find a similar activation energy for a process without any bulk diffusion.

The classical theory of nucleation assumes that the rate of island nucleation is proportional to c_{n^*} , where n^* is the critical cluster size at which adding one more atom decreases the free energy (i.e., $dE_{n^*}/dn = \mu$). Appreciable growth only occurs at supersaturations close to those needed for island nucleation, marked by the vertical lines in figure 7. Our observation is consistent with the conclusion that clusters (as subcritical nuclei) are becoming plentiful during growth (and that $n^* > \sim 5$).

3.5. Microscopic interpretation of cluster-attachment kinetics

Why, then, does graphene only grow from clusters of about five atoms and not the much more abundant monomers? The observed nonlinear growth kinetics suggests that attachment does not occur in one step. Instead, an intermediate (precursor) state must be thermally excited. Consider two possible interpretations: one is that C monomers must first break their strong bonds to the metal substrate—DFT calculations show that the monomer's lowest energy state is in the hcp 3-fold hollow site, 1.0 \AA above the plane through the centres of the Ru surface atoms. Thus, to attach to a graphene edge that lies at heights of up to 3.7 \AA [20] (see schematic in figure 9),

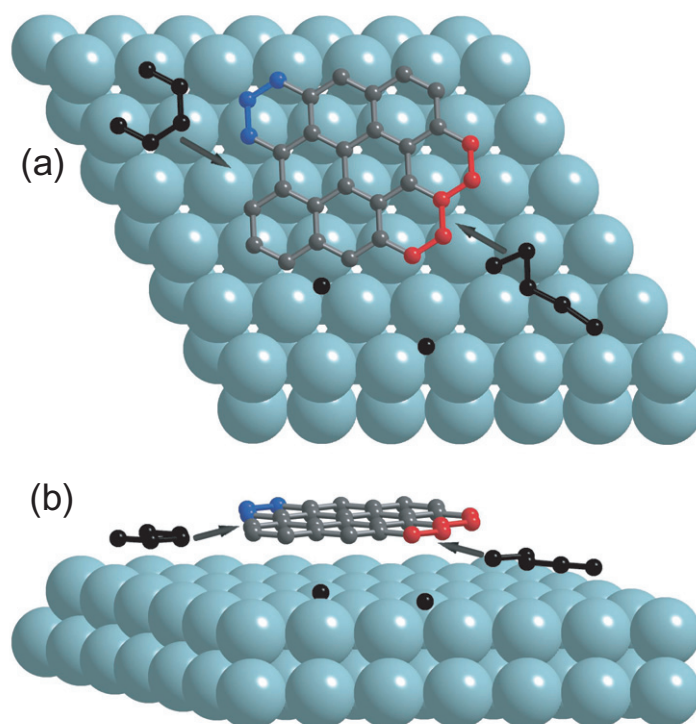


Figure 9. Schematic (a) top and (b) side views of graphene growth by attachment of C-atom clusters. Two 5-atom clusters (black) are sketched. Isolated C adatoms reside in the 3-fold hollow sites of the Ru substrate (green), $\sim 2 \text{ \AA}$ below the graphene sheet. At least three C atoms must be added to the *compact* graphene island (grey-shaded atoms) to form new six-membered rings. Adding three (blue) or five (red) C atoms makes one or two new six-membered rings, respectively.

C monomers must break strong bonds to three Ru atoms in the substrate. We speculate that this might explain why we observe a large barrier opposing C atom attachment to the graphene edge. The intermediate cluster state presumably involves both C–C and C–metal bonds, likely allowing the C to bridge the spatial and energetic gap between the deeply embedded C adatom and the much higher C atoms in the graphene. In this view, graphene grows by cluster addition on any substrate where C adatoms are strongly bound, e.g., on many metals. Indeed, simulations of graphene growth on Ni(111) provide evidence that three to five carbon-atom ‘chains’ are precursors to graphene growth [38].

In the above discussion, we have implicitly assumed that clusters are created uniformly over the Ru terraces. The second possibility is that the cluster forms only during the attachment event. Consider the compact graphene island of grey-shaded C atoms shown in figure 9. At least three C atoms must be added to the compact island to form new six-membered rings. But adding three carbon atoms produces an isolated ring (shown in blue), which may not provide a pathway to attachment because three of its C atoms are bonded only to two C atoms. In contrast, attaching five C atoms (red-shaded) to the compact island adds two adjacent six-membered rings. If this configuration is the smallest stable ‘nucleus’ for further island growth, then adding fewer C atoms would not grow graphene. Once this stable nucleus forms, a new ring can form along the row by adding just two C atoms. Thus, the crystal will rapidly grow

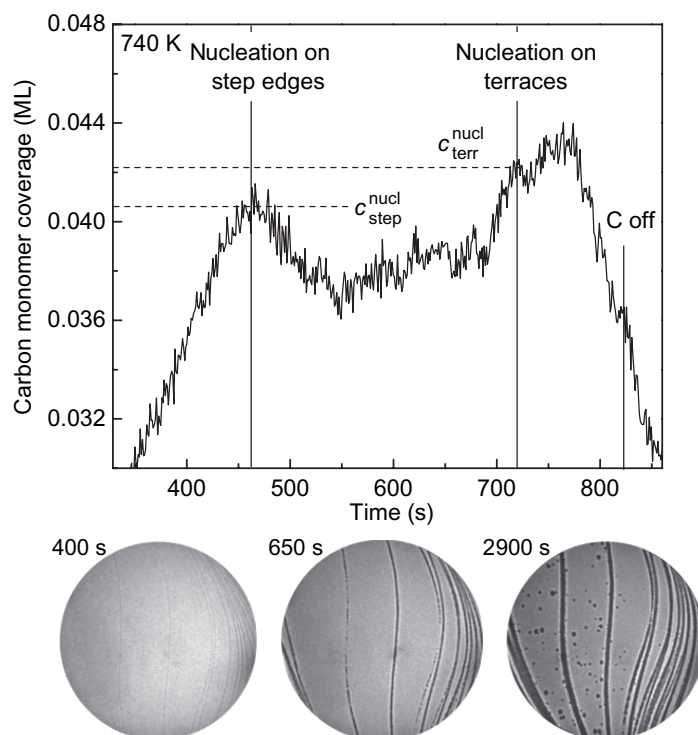


Figure 10. The time evolution of C monomer concentration during C deposition at 740 K. Graphene first nucleates at step edges of the Ru substrate when the monomer concentration reaches $c_{\text{step}}^{\text{nucl}}$. At higher concentration $c_{\text{terr}}^{\text{nucl}}$, graphene nucleates on the terraces. The deposition flux was reduced at 770 s and turned off at 830 s. LEEM images ($9.3 \mu\text{m}$ field-of-view) taken at the labelled times.

until reaching the next compact shape, where adding five C adatoms is again necessary to nucleate a new ‘riser’ along an island edge before further crystal growth can happen. The cluster addition illustrated schematically in figure 9 is very similar to growth mechanisms suggested for crystals with complex unit cells [19, 39]. Such ‘non-Kossel’ crystals must grow by the addition of atoms to inequivalent sites, or by the addition of clusters of atoms. (In contrast Kossel crystals grow by adding single atoms or molecules to a step-edge kink.) In fact, growth laws similar to equation (4) have been proposed for non-Kossel crystals [19]. Finding this behaviour in a simple material like graphene is surprising. In addition, the suggested mechanism of cluster addition bears similarities to proposed mechanisms of how graphene sheets grow from hydrocarbons during soot formation [1], where the requirement for breaking H–C bonds is analogous to breaking C–metal bonds.

3.6. Controlling graphene nucleation by monitoring C adatom supersaturation

We close by demonstrating that careful monitoring of supersaturation can be used to pattern growing graphene sheets. By controlling where graphene nucleates, one might manipulate the graphene morphology, for example, by predepositing patterns of preferred nucleation sites. However, careful control of supersaturation is required because growth occurs so close to the nucleation limit. Figure 10 shows how graphene nucleates only at substrate steps at

monomer concentration $c_{\text{step}}^{\text{nucl}}$. This initial step-edge nucleation is consistent with previous work [8, 11, 15] and with proposals that step edges lower the barrier to graphene nucleation [2]. At this temperature, graphene continues to decorate the step edge, forming graphene ribbons of uniform width. However, if the C monomer concentration is slightly increased to $c_{\text{terr}}^{\text{nucl}}$, multiple nucleation events are observed on the terraces. Defects within graphene sheets will occur at the boundaries where the separately nucleated islands impinge, which lead to the formation of highly defective graphene sheets. While $c_{\text{terr}}^{\text{nucl}} - c_{\text{step}}^{\text{nucl}}$ is very small, on the order of thousandths of a ML, our approach is precise enough to form these patterns controllably. In fact, using equation (3), the chemical potential difference of the monomer adatom gas between these two concentrations is only $kT \ln(c_{\text{step}}^{\text{nucl}}/c_{\text{terr}}^{\text{nucl}}) \approx 5$ meV, corresponding to a change in nucleation barrier of 30 meV, if $n^* = 6$. Thus, providing nucleation sites with a smaller nucleation barrier would make the patterning process easier.

4. Summary

In summary, we can control and measure the C monomer density during C deposition and at the same time measure the rate at which graphene grows. Thus, we obtain unique and direct information about the processes that determine the growth. Crystal growth can be diffusion limited (i.e., limited by the rate at which monomers diffuse towards the growing crystal) or attachment limited (i.e., limited by the rate at which atoms attach to the crystal). We find strong evidence for a large attachment barrier. Indeed, the attachment barrier is so substantial that growth occurs by cluster addition and is not in the linear regime that is commonly observed on metal and semiconductor surfaces. The large barrier to growth can be useful, allowing graphene morphology to be controlled by controlling the C supersaturation. Given that the barrier arises from a general characteristic of graphene, i.e., that on many substrates it is weakly bound compared with C adatoms, we anticipate that our conclusion that graphene needs a multiatom precursor for growth will hold for other types of deposition and other substrates.

Acknowledgments

We thank J C Hamilton, J J de Yoreo and T Ohta for helpful discussions. This work was supported by the Office of Basic Energy Sciences, Division of Materials Sciences of the US DOE under contract DE-AC04-94AL8500. VASP was developed at T U Wien's Institut für Theoretische Physik.

References

- [1] Whitesides R, Kollias A C, Domin D, Lester W A Jr and Frenklach M 2007 Graphene layer growth: collision of migrating five-membered rings *Proc. Combust. Inst.* **31** 539–46
- [2] Bengaard H S, Norskov J K, Sehested J, Clausen B S, Nielsen L P, Molenbroek A M and Rostrup-Nielsen J R 2002 Steam reforming and graphite formation on Ni catalysts *J. Catal.* **209** 365–84
- [3] Hofmann S, Csanyi G, Ferrari A C, Payne M C and Robertson J 2005 Surface diffusion: the low activation energy path for nanotube growth *Phys. Rev. Lett.* **95** 036101
- [4] Helveg S, Lopez-Cartes C, Sehested J, Hansen P L, Clausen B S, Rostrup-Nielsen J R, Abild-Pedersen F and Norskov J K 2004 Atomic-scale imaging of carbon nanofibre growth *Nature* **427** 426–29

- [5] Berger C *et al* 2006 Electronic confinement and coherence in patterned epitaxial graphene *Science* **312** 1191–96
- [6] Klusek Z *et al* 2005 Local electronic edge states of graphene layer deposited on Ir(111) surface studied by STM/CITS *Appl. Surf. Sci.* **252** 1221–27
- [7] Mallet P, Varchon F, Naud C, Magaud L, Berger C and Veuillen J Y 2007 Electron states of mono- and bilayer graphene on SiC probed by scanning-tunneling microscopy *Phys. Rev. B* **76** 041403
- [8] Sutter P W, Flege J-I and Sutter E A 2008 Epitaxial graphene on ruthenium *Nat. Mater.* **7** 406–11
- [9] Hibino H, Kageshima H, Maeda F, Nagase M, Kobayashi Y and Yamaguchi H 2008 Microscopic thickness determination of thin graphite films formed on SiC from quantized oscillation in reflectivity of low-energy electrons *Phys. Rev. B* **77** 075413
- [10] Coraux J, N'Diaye A T, Busse C and Michely T 2008 Structural coherency of graphene on Ir(111) *Nano Lett.* **8** 565–70
- [11] Marchini S, Gunther S and Wintterlin J 2007 Scanning tunneling microscopy of graphene on Ru(0001) *Phys. Rev. B* **76** 075429
- [12] Oshima C and Nagashima A 1997 Ultra-thin epitaxial films of graphite and hexagonal boron nitride on solid surfaces *J. Phys.: Condens. Matter* **9** 1–20
- [13] Rutter G M, Crain J N, Guisinger N P, Li I, First P N and Stroscio J A 2007 Scattering and interference in epitaxial graphene *Science* **317** 219–22
- [14] Shelton J C, Patil H R and Blakely J M 1974 Equilibrium segregation of carbon to a nickel (111) surface—surface phase-transition *Surf. Sci.* **43** 493–520
- [15] Wu M C, Xu Q and Goodman D W 1994 Investigations of graphitic overlayers formed from methane decomposition on Ru(0001) and Ru(11(2)over-Bar-0) catalysts with scanning-tunneling microscopy and high-resolution electron energy loss spectroscopy *J. Phys. Chem.* **98** 5104–10
- [16] Ohta T, El Gabaly F, Bostwick A, McChesney J L, Emtsev K V, Schmid A K, Seyller T, Horn K and Rotenberg E 2008 Morphology of graphene thin film growth on SiC(0001) *New J. Phys.* **10** 023034
- [17] Land T A, Michely T, Behm R J, Hemminger J C and Comsa G 1992 Stm investigation of single layer graphite structures produced on Pt(111) by hydrocarbon decomposition *Surf. Sci.* **264** 261–70
- [18] Lindroos M, Pfnur H and Menzel D 1986 Theoretical and experimental-study of the unoccupied electronic band-structure of Ru(001) by electron reflection *Phys. Rev. B* **33** 6684–93
- [19] Chernov A A 2004 Notes on interface growth kinetics 50 years after Burton, Cabrera and Frank *J. Cryst. Growth* **264** 499–518
- [20] Wang B, Bocquet M-L, Marchini S, Gunther S and Wintterlin J 2008 Chemical origin of a graphene moiré overlayer on Ru(0001) *Phys. Chem. Chem. Phys.* **10** 3530–34
- [21] de la Figuera J, Bartelt N C and McCarty K F 2006 Electron reflectivity measurements of Ag adatom concentrations on W(110) *Surf. Sci.* **600** 4062–66
- [22] Kresse G and Hafner J 1994 Ab-initio molecular-dynamics simulation of the liquid-metal amorphous-semiconductor transition in germanium *Phys. Rev. B* **49** 14251–69
- [23] Kresse G and Hafner J 1993 Ab initio molecular-dynamics for liquid-metals *Phys. Rev. B* **47** 558–61
- [24] Perdew J P, Chevary J A, Vosko S H, Jackson K A, Pederson M R, Singh D J and Fiolhais C 1992 Atoms, molecules, solids, and surfaces: applications of the generalized gradient approximation for exchange and correlation *Phys. Rev. B* **46** 6671
- Perdew J P, Chevary J A, Vosko S H, Jackson K A, Pederson M R, Singh D J and Fiolhais C 2003 *Phys. Rev. B* **48** 4978 (erratum)
- [25] Blochl P E 1994 Projector augmented-wave method *Phys. Rev. B* **50** 17953–74
- [26] Kresse G and Joubert D 1999 From ultrasoft pseudopotentials to the projector augmented-wave method *Phys. Rev. B* **59** 1758–75
- [27] Neugebauer J and Scheffler M 1992 Adsorbate-substrate and adsorbate-adsorbate interactions of Na and K adlayers on Al(111) *Phys. Rev. B* **46** 16067–80

- [28] Martoccia D, Willmott P R, Brugger T, Björck M, Günther S, Schlepütz C M, Cervellino A, Pauli S A, Patterson B D, Marchini S, Wintterlin J, Moritz W and Greber T 2008 Unit cell of graphene on Ru(0001): a 25×25 supercell with 1250 carbon atoms arXiv:0808.1853v1
- [29] Shimizu T K, Mugarza A, Cerdá J I, Heyde M, Qi Y, Schwarz U D, Ogletree D F and Salmeron M 2008 Surface species formed by the adsorption and dissociation of water molecules on a Ru(0001) surface containing a small coverage of carbon atoms studied by scanning tunneling microscopy *J. Phys. Chem. C* **112** 7445–54
- [30] Tontegode A Y 1991 Carbon on transition metal surfaces *Prog. Surf. Sci.* **38** 201–429
- [31] Koskinen P, Malola S and Häkkinen H 2008 Self-passivating edge reconstructions of graphene *Phys. Rev. Lett.* **101** 115502
- [32] Jeong H C and Williams E D 1999 Steps on surfaces: experiment and theory *Surf. Sci. Rep.* **34** 171–294
- [33] Giesen M 2001 Step and island dynamics at solid/vacuum and solid/liquid interfaces *Prog. Surf. Sci.* **68** 1–153
- [34] Yazyev O V and Pasquarello A 2008 Effect of metal elements in catalytic growth of carbon nanotubes *Phys. Rev. Lett.* **100** 156102
- [35] Bartelt N C and Tromp R M 1996 Low-energy electron microscopy study of step mobilities on Si(001) *Phys. Rev. B* **54** 11731–40
- [36] Chernov A A 1989 Formation of crystals in solutions *Contemp. Phys.* **30** 251–76
- [37] Kaatz F H, Siegal M P, Overmyer D L, Provencio P P and Tallant D R 2006 Thermodynamic model for growth mechanisms of multiwall carbon nanotubes *Appl. Phys. Lett.* **89** 241915
- [38] Amara H, Bichara C and Ducastelle F 2006 Formation of carbon nanostructures on nickel surfaces: a tight-binding grand canonical Monte Carlo study *Phys. Rev. B* **73** 113404
- [39] Rashkovich L N, De Yoreo J J, Orme C A and Chernov A A 2006 *In situ* atomic force microscopy of layer-by-layer crystal growth and key growth concepts *Crystallogr. Rep.* **51** 1063–74